

## Layer-by-layer growth of solid argon films on graphite as studied by neutron diffraction

J. Z. Larese, Q. M. Zhang, L. Passell, and J. M. Hastings  
*Brookhaven National Laboratory, Upton, New York 11973*

J. R. Dennison\* and H. Taub

*Department of Physics, University of Missouri-Columbia, Columbia, Missouri 65211*

(Received 10 April 1989)

The layer-by-layer growth of solid argon films on graphite at  $T=10$  K is studied using elastic neutron diffraction. The growth is characterized by individual layers with commensurate in-plane lattice constants. As the coverage is increased beyond two layers, evidence of the coexistence of *ABC* and *ABA* stacking is apparent, with the *ABC* sequence dominating as the film thickens. A continuous decrease in the Debye-Waller factor also occurs as the film thickness grows, indicating a crossover from two-dimensional to three-dimensional behavior. As the coverage is increased beyond about four nominal layers, there is evidence of bulk crystallite formation. The diffraction results are compared with equivalent measurements for methane films and with the recent computer simulations of Hruska and Phillips.

Understanding the basic mechanisms which govern the microscopic growth of multilayer films on solid surfaces is a problem which poses a tremendous challenge to the surface scientist. It is widely recognized that the number of uniform layers which form on a surface is finite if the structural parameters of the film differ significantly from those of the bulk solid (i.e., *incomplete* wetting occurs). Hence, it seems reasonable to assume that a detailed knowledge of the microscopic arrangement within the first few layers of a thin film is crucial for understanding why wetting does or does not occur. Our purpose here is to use neutron diffraction to determine the structural properties of thin solid argon films (one to four layers thick) physisorbed on a graphite substrate, and to compare them with equivalent data for solid methane films on graphite. We chose these two systems because previous theoretical predictions<sup>1</sup> and experimental evidence<sup>2,3</sup> suggested that under appropriate conditions complete wetting (i.e., infinite layer-by-layer growth) occurs. The recent availability of computer simulations<sup>4,5</sup> for these systems has greatly aided our study of the microscopic layering process. Comparing our neutron scattering results with the simulations opens an avenue for answering questions not previously possible by diffraction methods alone. We view these combined microscopic studies as a necessary first step in understanding multilayer film growth and such related phenomena as surface roughening and premelting, the sintering of bulk solids, and interfacial melting.

In a previous study,<sup>6</sup> we calculated the powder-averaged diffraction profiles for a model system consisting of close-packed scatterers with either an *ABC* or *ABA* stacking sequence. Figure 1 shows the thickness dependence of the low-angle diffraction pattern for such an idealized system, i.e., one in which there is no sub-

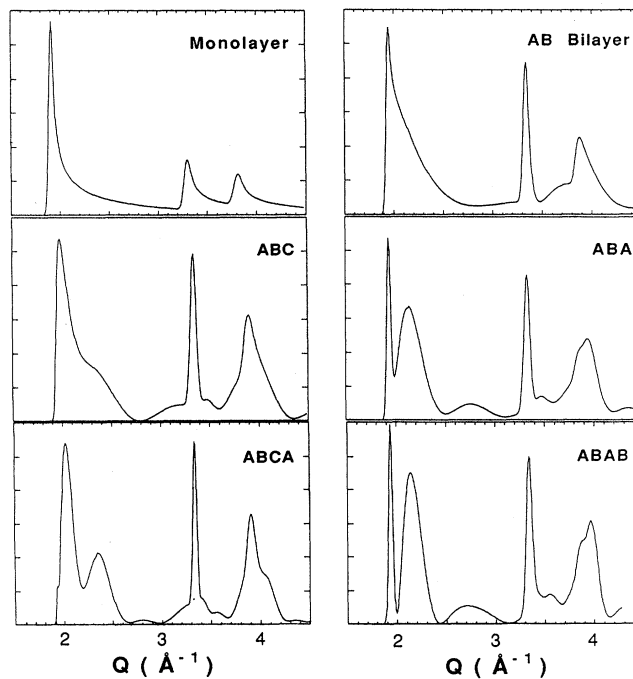


FIG. 1. Model line-shape calculations of powder-averaged diffraction profiles for an ideal system of close packed scatterers. A direct comparison is made of the two possible stacking sequences (i.e., *ABC* and *ABA*) as a function of layer thickness. All in-plane structures are commensurate, triangular, and chosen to have the same nearest-neighbor separation of 3.76 Å. The fixed interplane distance of 3.07 Å was used for all calculations. The figures shown include the effects of folding a Gaussian instrument function (with a full width at half maximum of  $\approx 0.03$  Å<sup>-1</sup>) in order to illustrate what would be recorded in an idealized experiment.

strate. This simplified picture of the layering process can serve, however, as a conceptual basis for more detailed investigations. The actual atomic arrangement within a film several layers thick is unquestionably more complicated because real physical systems have stacking faults, domain walls, and other imperfections which result from the presence of surface steps, inhomogeneities, impurities, vacancies, etc. In fact, even in a model system of close-packed spheres, structural incompatibilities can occur because two stacking sequences (i.e., *ABA* and *ABC*) are possible. For most systems, but more specifically for argon on graphite, the difference in formation energy between *ABA* and *ABC* stacking is essentially indistinguishable<sup>7</sup> making it difficult to predict, *a priori*, which stacking sequence will dominate in the thin-film (three to four layer) regime. Most theoretical treatments of argon film growth to date have used the *ABC* stacking sequence as their starting point, assuming that it represents the lowest-energy configuration of the system. This constraint seems justified since bulk solid argon forms an fcc structure<sup>8</sup> and in order for an argon film to attain macroscopic size (i.e., completely wet the graphite), the *ABC* sequence must ultimately dominate. Previous electron diffraction studies using a single-crystal graphite substrate<sup>2</sup> have indicated that solid argon films completely wet at low temperatures, although no indication of the lattice constants or stacking arrangement was given. However, a more recent, higher-temperature thermodynamic study of this layering process employing a

graphite fiber oscillator,<sup>9</sup> suggests that only a finite number of argon layers can form before bulk condensation occurs. The results of this thermodynamic study are consistent with triple-point wetting for the argon-graphite system. A direct determination of the structural parameters of the argon multilayer system may therefore prove valuable in helping to understand where the origin of this discrepancy lies.

Phillips and co-workers have recently performed several Monte Carlo computer simulations<sup>4</sup> from which they abstracted equilibrium *snapshots* of the atomic arrangements within argon and methane-on-graphite multilayer films. The interplay between computer simulations and neutron experiments has been of benefit to both groups by suggesting realistic models of the argon-graphite growth process.

The neutron scattering experiments were performed at the Brookhaven National Laboratory-High-Flux-Beam Reactor (HFBR) on the *H5* triple-axis spectrometer. Scans were made with the spectrometer operating in the elastic mode at a wavelength of either 1.64 or 2.43 Å with a  $Q$  (wave-vector) resolution of  $\approx 0.03 \text{ \AA}^{-1}$  FWHM. Research grade <sup>36</sup>Ar gas was used as the adsorbant because this particular isotope has a large coherent scattering cross section. The substrate, a vermicular form of crystalline graphite,<sup>10</sup> was formed into several cylindrical pieces (by recompressing the powder), before placing it in a thin-walled aluminum cell. The sample cell was mounted on the cold finger of a closed-cycle helium refrigerator,

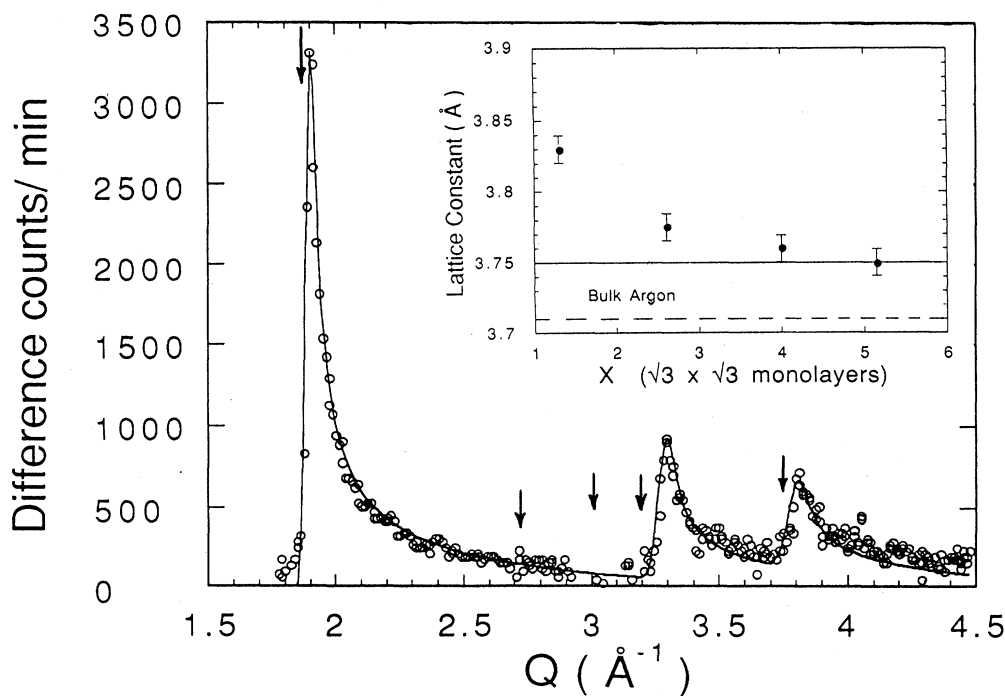


FIG. 2. Typical monolayer difference profile (open circles) from an  $X = 1.3$  film of <sup>36</sup>Ar film on vermicular graphite at 10 K. The solid line fit is a powder-averaged fit to an incommensurate triangular solid with lattice constant of 3.830 Å and a Debye-Waller factor of 0.055 Å<sup>2</sup>. The arrows indicate the regions on the difference spectrum where background diffraction signals from the graphite substrate and aluminum sample cell appear. The inset shows the lattice compression as a function of coverage at 10 K. The solid and dashed lines in the inset are extrapolations of the bulk argon lattice constant at  $\approx 10$  K from previous x-ray and neutron diffraction studies referenced in the text, respectively.

whose temperature was regulated to better than 0.05 K. As in previous experiments, all surface coverages,  $X$ , are in units such that  $X = 1.00$  corresponds to one complete register  $\sqrt{3} \times \sqrt{3}$  monolayer as determined from a nitrogen isotherm performed at  $T = 77.0$  K. All the argon films were first annealed at  $T \approx 90$  K and then at  $T \approx 70$  K for about 2 h at each temperature, then slowly cooled (about 1 K/min) to 10 K. It should be noted that the sample cell and capillary fill-line arrangement used in the present experiments was redesigned in order to eliminate problems with long equilibration times experienced in our previous studies of thick methane films ( $X > 3.5$ ). The new arrangement eliminates a relatively large volume bellows valve, which was located in a low-temperature portion of the cryostat.

Figure 2 shows a typical monolayer diffraction profile which, as usual, has had the substrate-sample cell background subtracted. The solid-line fit to the data is the result of a powder-averaged profile characteristic of an incommensurate, triangular two-dimensional (2D) solid convoluted with a Gaussian instrument response function.<sup>11</sup> The high quality of the fit gives us confidence that our line-fitting procedure accurately describes the data. Perhaps the most serious drawback in experiments of this type is the presence of the intense graphite (002) background reflection in the immediate neighborhood of the lowest-order (10) film peak. Although this graphite peak becomes less significant as the argon layers are compressed (since the compressions moves the diffracted peak to a higher-scattering angle), it nonetheless complicates the interpretation of the data in the vicinity of  $Q \approx 1.87 \text{ \AA}^{-1}$ . Additional complications caused by the small shifts in the graphite (002) peak position and changes in peak shape produced by the addition of argon layers have been discussed previously.<sup>12</sup>

The inset in Fig. 2 illustrates how the lattice constant varies with surface coverage. A gradual decrease in the nearest-neighbor distance (which asymptotically approaches the bulk value<sup>8</sup>) is observed. In all cases the triangular solid that forms is incommensurate with the graphite substrate. These results differ dramatically from the behavior observed in an equivalent study of adsorbed methane films. In that study we observed a compression of the methane nearest-neighbor distance to a value which was about 1% smaller than the bulk lattice constant. Recent theoretical investigations<sup>13</sup> of adsorbed methane monolayer over-compression predict a lattice constant in good agreement with the experimental value.

As the surface coverage is increased beyond monolayer completion (i.e.,  $X > 1.4$ ), evidence of monolayer and bilayer solid coexistence is clearly seen in the diffraction profiles. Excellent fits in this coverage regime were obtained by using a monolayer-bilayer coexistence, but will not be shown here since we plan to present them in a future, longer report.

Figures 3(a) and 3(b) display the diffraction profiles close to bilayer and trilayer completion, respectively. The solid-line fit to the bilayer diffraction profile was obtained by varying the in-plane and inter-plane distances, but with the individual layers constrained to be commensurate with one another. A sensitivity of better than

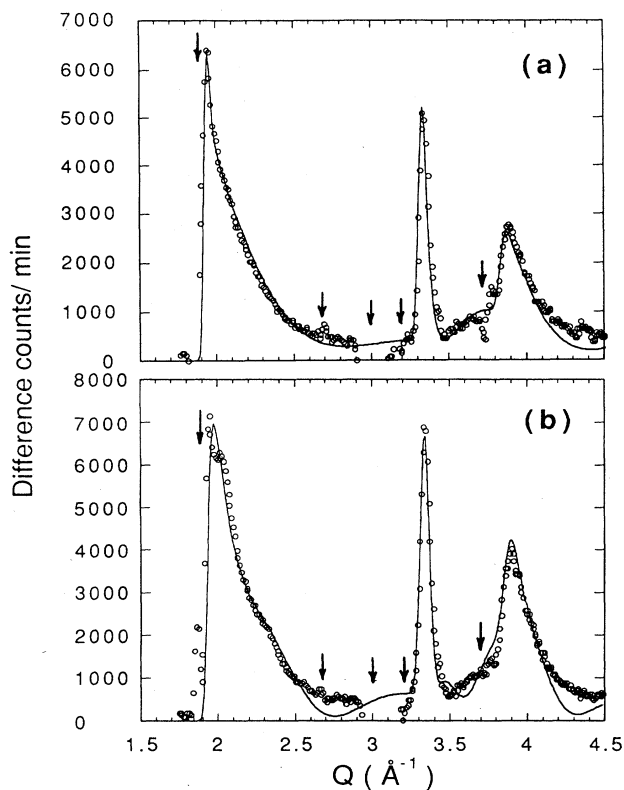


FIG. 3. (a) Diffraction profile recorded for  $X = 2.61$  monolayer solid  $^{36}\text{Ar}$  film recorded at 10 K. The solid line represents a fit to a triangular  $AB$  bilayer structure using the same nearest-neighbor distance of  $3.775 \text{ \AA}$  for each layer and interlayer spacing of  $3.17 \text{ \AA}$ . A  $0.045 \text{ \AA}^2$  Debye-Waller factor was used in the fit. (b) Diffraction profile recorded for  $X = 4.00$  monolayer solid  $^{36}\text{Ar}$  film recorded at 10 K. The solid line represents a fit to the data assuming a composite line shape constructed by combining both  $ABC$  and  $ABA$  stacking sequences with a contribution of 85 and 15%, respectively. A nearest-neighbor distance of  $3.760 \text{ \AA}$ , an interlayer spacing of  $3.20 \text{ \AA}$ , and a  $0.030 \text{ \AA}^2$  Debye-Waller factor was used in the fit. The arrows indicate the regions in both spectra where background diffraction signals from the graphite substrate and aluminum sample cell appear.

0.5% for the in-plane distance and 5% for the inter-plane distance is realized with the current instrument resolution. A spatial correlation range  $> 300 \text{ \AA}$  (a value consistent with the crystallite size of the vermiculite substrate) and a  $0.045 \text{ \AA}^2$  Debye-Waller factor was used to obtain the fit shown in the figure. The argon lattice compresses slightly with the addition of the second layer as expected, but does not contract beyond the bulk value. These results are once again strikingly different from those obtained for the bilayer methane solid. In the methane study it was found that the individual solid layers were incommensurate with one another. Both the argon and methane diffraction studies are in excellent agreement with computer simulations of their microscopic structure made by Hruska and Phillips. In that study, the 2D pair distribution function for the first two layers

of argon films on graphite were found to be identical, whereas for an equivalent methane bilayer the 2D pair distribution functions for the two layers differed significantly. This led Hruska and Phillips to conclude that in the bilayer argon solid the individual layers would form in registry with one another while in the methane bilayer the two layers would be incommensurate, exactly as observed in the neutron experiments.

The diffraction data for the trilayer film in Fig. 3(b) can be best fit by a model line shape which assumes regions of *ABA* (15%) and *ABC* (85%) stacking, as illustrated by the solid line in the figure. In light of our opening remarks, the coexistence of the two stacking sequences is not unexpected. Additional support for our suggestion that a typical three-layer film is composed of *ABC* and *ABA* regions can be obtained by considering that both, the packing fraction, and the coordination number for these two stacking arrangements are the same. This suggests that an appreciable energy difference in the adatom-adatom interaction only shows up at the next-nearest-neighbor level. In a three-layer system only a small fraction of the atoms have all of their next nearest neighbors (i.e., in the 3D sense) lending further support to the suggestion that both stacking sequences should coexist. A fit to the data assuming a pure *ABC* model is fair but a pure *ABA* model fails miserably (see Fig. 1). In fact, if in addition to assuming that we need a combination of the two stacking sequences, we also include a small amount of bilayer component, the fit becomes even better. Since we are at a coverage which is roughly 95% of that needed for trilayer completion, it is not surprising that this is necessary. But the introduction of additional fitting parameters simply complicates the analysis without adding anything to the physical understanding of the growth process. In our earlier work with methane<sup>6</sup> roughly 20% more molecules, beyond the value determined from the lattice constant of the *n*th-layer solid, were necessary in order to complete that layer. This suggests that in cases where a compression of an *n*-layer solid occurs, some small (but significant) number of atoms will probably occupy the *n* + 1, *n* + 2, . . . layer (or layers). What the fractional population of each layer will be, of course, depends on the details of the gas-solid interaction and the temperature.<sup>14</sup>

Our results are in good agreement with the most recent computer simulations of Phillips.<sup>5</sup> In the three-layer regime at low temperatures, his computer *snapshots* show definite patches of *ABC* and *ABA* stacking, and a small but finite population of atoms in higher layers. As with the monolayer and bilayer solids, the spatial coherence length of the trilayer solid is found to be about 300 Å. Interestingly, a further decrease in the Debye-Waller factor to 0.03 Å<sup>2</sup> is necessary to fit the data, indicating that the three-layer solid is distinctly more rigid than its monolayer or bilayer equivalent.

The diffraction profile of a film near four-layer completion still indicates the need for a model with *ABA* and *ABC* components. In this case, however, an increase in the fractional amount of the *ABC* component is necessary. This behavior is consistent with the tendency of the film to prefer the *ABC* stacking arrangement found in

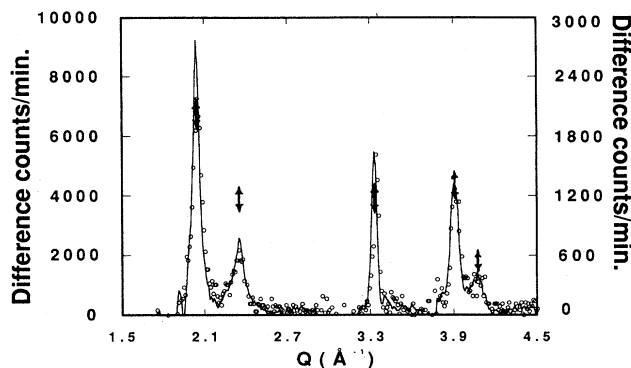


FIG. 4. Difference traces which illustrate the growth of bulk solid argon crystallites at 10 K produced by taking the difference between the scattering recorded at  $X=5.5$  and  $5.15$  (open circles) and the difference between  $X=8.07$  and  $5.15$  (solid line). The solid arrows indicate the expected position and intensity for a bulk argon powder diffraction pattern. It should be noted that the left- and right-hand scales differ by a factor of  $\approx 3.3$ .

bulk argon. The computer simulations for film densities near this coverage also indicate an increased preference for forming the *ABC* structure. It is also important to point out that a continued further reduction in the Debye-Waller factor to 0.02 Å<sup>2</sup> is necessary to fit the four-layer data properly, indicating a continued stiffening of the four-layer solid. Furthermore, the in-plane lattice constant does not compress to the bulk value and the interplane distance remains larger than that expected for close packing.

Figure 4 shows the spectra which result from subtracting a scan taken at  $X=5.1$  from those recorded at  $X=5.5$  and  $8.07$ . The arrows locate the predicted peak positions and intensities for a bulk argon powder diffraction scan [scaled to the (111) reflection] superimposed on the *Gaussian*-shaped difference peaks. Although the distinction between a bulk powder-diffraction line shape and that of a layered film diminishes as the number of layers increases, model calculations suggest that this distinction is still easily discernible at six layers. Using the model calculations presented in Fig. 1, and assuming a film thickness within the range of four to seven layers, we calculated a difference trace for every possible combination of four- to seven-layer model shapes (i.e., *ABCABCA-ABCABC*, *ABCABCA-ABCAB*, *ABCABC-ABCA*, etc.). The resulting traces were quite different from the one shown in Fig. 4 with regard to both the positions and shapes of the peaks. On the other hand, the good agreement of this pattern, with that calculated for bulk solid argon and the near perfect scaling of the difference spectra shown in Fig. 4, as the coverage is increased from  $X=5.15$  to  $8.07$ , leads us to suspect that once four or five nominal layers of solid film are on the surface, the formation of bulk crystallites has already begun via capillary condensation [in fact, a near perfect fit to the four-layer data profile can be obtained if a small amount of bulk ( $\approx 4\%$ ) signal is added]. Capillary con-

densation would also explain why the vapor-pressure measurements performed during a recent thermodynamic study of argon multilayers<sup>15</sup> converged fairly slowly to the expected bulk vapor-pressure value  $P_0$ . The certainty with which we can make this statement is limited by the fact that the layered film approaches bulk density as the coverage is increased (see, e.g., inset to Fig. 4). In this respect the argon-on-graphite system differs from other systems where incomplete wetting has been clearly identified ( $O_2$ ,  $N_2$ ,  $C_2H_4$ ) since, in the latter, the film and bulk components are different enough in structure so that they can be easily identified in the diffraction patterns. Even though the present data tends to support the hypothesis that bulk crystallites form at higher coverages, a word of caution with regard to the wetting properties of argon on graphite is necessary. The evidence of bulk argon formation, which appears in our experimental profiles, may *not* accurately address the issue of whether or not solid argon *intrinsically* prefers to wet graphite completely at low temperatures. It may only indicate that the morphology of the graphite used in these experiments determines the adsorption behavior when the number of atoms (or layers) in the cell exceeds some particular substrate-sample dependent value, i.e., bulk formation may not be an intrinsic property of the system. On the other hand, since the measured interlayer distances have not attained the bulk value even at four-layer thickness, it is possible that the substrate interaction is too weak to support further layer compression, and there is enough vertical strain to impede further uniform layering. This, of course, means that experiments performed with a single-crystal graphite substrate might ultimately be more reliable in determining the wetting behavior of a particular surface than those performed with a powder-type substrate. X-ray studies using single-crystal substrates are planned to address this issue.

In conclusion we have demonstrated that the growth of solid argon films on graphite can be studied with conventional neutron powder-diffraction techniques. The data establish layer-by-layer growth of argon on graphite (to at least four layers) and provide an interesting contrast with the behavior of methane in the one to three layer regime. Excellent agreement is found with the diffraction line shapes predicted from simple close-packed models and with the results of computer simulations. As the thickness of the film decreases the systematic increase in the observed Debye-Waller factor is consistent with a softening of the elastic constants as the system dimensionality changes from 3D to 2D. An increase in the mean-square deviations of atoms from their equilibrium positions in systems of lower dimensionality<sup>16</sup> is a feature which has long been predicted to occur. These results should also be relevant to the interpretation of recent thermodynamic studies of the melting of thick films of argon<sup>15</sup> and methane<sup>17</sup> on graphite.

#### ACKNOWLEDGMENTS

We are very happy to acknowledge extensive and fruitful discussions with Jim Phillips at the University of Missouri-Kansas City whose computer simulations helped us "visualize" some of the film structures whose diffraction profiles we were observing. We have also benefited from helpful conversations with Ai-lan Cheng, Greg Dash, Walter Kunmann, and Bill Steele. Work performed at Brookhaven is supported by the U.S. Department of Energy, Division of Material Sciences under Contract No. DE-AC02-76CH00016. Work performed at the University of Missouri is supported by Grant No. DMR-8704938 from the National Science Foundation.

\*Present address: Department of Physics, Utah State University, Logan, UT 84322.

<sup>1</sup>J. M. Phillips, Phys. Rev. B **34**, 2823 (1986).

<sup>2</sup>J. L. Seguin, J. Suzanne, and M. Bienfait, J. G. Dash, and J. A. Venables, Phys. Rev. Lett. **51**, 122 (1983); E. Lerner, F. Hanons, and C. E. N. Gatts, Surf. Sci. **160**, L524 (1985).

<sup>3</sup>J. M. Gay, A. Dutheil, J. Krim, and J. Suzanne, Surf. Sci. **177**, 25 (1986); J. Krim, J. M. Gay, J. Suzanne, and E. Lerner, J. Phys. (Paris) **47**, 1757 (1986).

<sup>4</sup>C. Hruska and J. M. Phillips, Phys. Rev. B **37**, 3801 (1988).

<sup>5</sup>J. M. Phillips, Langmuir (to be published).

<sup>6</sup>J. Z. Lares, M. Harada, L. Passell, J. Krim, and S. Satija, Phys. Rev. B **37**, 4735 (1988).

<sup>7</sup>A. L. Cheng and W. A. Steele, Langmuir **5**, 600 (1989).

<sup>8</sup>D. G. Henshaw, Phys. Rev. **6**, 1470 (1958); E. R. Dobbs, B. F. Figgins, G. O. Jones, D. C. Piercy, and D. P. Riley, Nature **178**, 483 (1956).

<sup>9</sup>L. Brushi, G. Torzo, and M. H. W. Chan, Eur. Phys. Lett. B **6**, 541 (1988).

<sup>10</sup>Vermicular graphite is a product of the Union Carbide Company.

<sup>11</sup>G. J. Trott, H. Taub, F. Y. Hansen, and H. R. Danner, Chem. Phys. Lett. **78**, 504 (1981); G. J. Trott, Ph.D. thesis, University of Missouri, 1981.

<sup>12</sup>H. Taub, K. Carneiro, J. K. Kjems, L. Passell, and J. P. McTague, Phys. Rev. B **16**, 4551 (1977).

<sup>13</sup>L. W. Bruch, J. Chem. Phys. **87**, 5518 (1987).

<sup>14</sup>W. A. Steele, J. Colloid Interface Sci. **75**, 13 (1980).

<sup>15</sup>D. M. Zhu and J. G. Dash, Phys. Rev. Lett. **60**, 432 (1988); **57**, 2959 (1986).

<sup>16</sup>R. E. Peierls, Ann. Inst. Henri Poincaré **5**, 1771 (1935).

<sup>17</sup>J. J. Hamilton and D. L. Goodstein, Phys. Rev. B **28**, 3838 (1983).